Earth Syst. Dynam., 3, 87–96, 2012
www.earth-syst-dynam.net/3/87/2012/
doi:10.5194/esd-3-87-2012

Earth System Dynamics

The influence of vegetation on the ITCZ and South Asian monsoon in HadCM3

M. P. McCarthy[1], J. Sanjay[2], B. B. B. Booth[1], K. Krishna Kumar[2], and R. A. Betts[1]

[1]Met Office, Hadley Centre, Fitzroy Road, Exeter, EX12NY, UK
[2]Indian Institute of Tropical Meteorology, Pashan, Pune, 411008, India

Correspondence to: M. P. McCarthy (mark.mccarthy@metoffice.gov.uk)

Received: 20 December 2011 – Published in Earth Syst. Dynam. Discuss.: 6 February 2012
Revised: 9 May 2012 – Accepted: 22 May 2012 – Published: 22 June 2012

Abstract. The role of global vegetation on the large-scale tropical circulation is examined in the version 3 Hadley Centre climate model (HadCM3). Alternative representations of global vegetation cover from observations and a dynamic global vegetation model (DGVM) were used as the land-cover component for a number of HadCM3 experiments under a nominal present day climate state, and compared to the simulations using the standard land cover map of HadCM3. The alternative vegetation covers result in a large scale cooling of the Northern Hemisphere extra-tropics relative to the HadCM3 standard, resulting in a southward shift in the location of the inter-tropical convergence zone (ITCZ). A significant reduction in Indian monsoon precipitation is also found, which is related to a weakening of the South Asian monsoon circulation, broadly consistent with documented mechanisms relating to temperature and snow perturbations in the Northern Hemisphere extra-tropics in winter and spring, delaying the onset of the monsoon.

The role of the Northern Hemisphere extra-tropics on tropical climate is demonstrated, with an additional representation of vegetation cover based on DGVM simulated changes in Northern Hemisphere vegetation from the end of the 21st Century. This experiment shows that through similar processes the simulated extra-tropical vegetation changes in the future contribute to a strengthening of the South Asian monsoon in this model. These findings provide renewed motivation to give careful consideration to the role of global scale vegetation feedbacks when looking at climate change, and its impact on the tropical circulation and South Asian monsoon in the latest generation of Earth System models.

1 Introduction

An important aspect of climate research is to identify potential feedbacks and assess if such feedbacks could produce large and undesired responses to perturbations resulting from human activities (Denman et al., 2007). A significant driver of the climate research effort has focused on incorporation and quantification of the complex climate atmosphere-ocean-biosphere interactions within climate model frameworks. One particular area which has received greater attention in the past decade has been the representation of the land surface; motivated by the recognition of the potential for dramatic reductions in future carbon uptake into land carbon stores (Cox et al., 2000; Friedlingstein et al., 2006). While the focus of this model development has been largely aimed at improved modelling of land-atmosphere carbon exchange, this development has also lead to more sophisticated representations of the land surface characteristics within climate models. A number of models now dynamically model vegetation distributions (e.g. Cox, 2001; Levis et al., 2004; Gallimore et al., 2005; Jones et al., 2011) where the fraction of tree and grass species is a function of the local climate state. Previously, climate models needed to prescribe vegetation coverage. The strength of this new approach is that future changes in vegetation extent can now be represented explicitly. For example Cox et al. (2000) demonstrated the potential for large scale Amazonian forest loss due to changes in projected rainfall, promoting continued research into both the resilience and response of tropical forests to climate change (Malhi et al., 2009).

In this study we examine climate and vegetation in experiments performed using the Hadley Centre global atmosphere-ocean climate model, HadCM3, coupled to a dynamic global vegetation model (DGVM). The analysis was initially motivated by noting a significant decline in precipitation over India during the South Asian monsoon in an ensemble of simulations of the carbon-cycle version of HadCM3 (below and Booth et al., 2012) when compared with an ensemble of the standard HadCM3 configuration without the carbon cycle. It has been demonstrated in other studies that HadCM3 is able to reasonably simulate the mean monsoon and seasonality (e.g. Martin et al., 2000; Turner and Slingo, 2009), so it is therefore of some value to determine what aspect of the carbon-cycle version of the model contribute to degrading this.

Previous studies using different versions of this model had indicated that the land use and land cover change did not significantly affect climate at the regional and local scales (e.g. Lawrence and Slingo, 2004; Osborne et al., 2004; Crucifix et al., 2005). Using the atmospheric component of this model, Lawrence and Slingo (2004) found little difference in climate simulations that use annual mean vegetation characteristics compared with those that use a prescribed seasonal cycle. Osborne et al. (2004) used a similar version and assessed the influence of vegetation in the tropics by comparing the results of integrations with and without tropical vegetation. Their results indicated that in the tropics vegetation produced variability in surface fluxes and their coupling to precipitation. However, Osborne et al. (2004) found significant regional variations in the feedback of vegetation on the local precipitation. For example, the state of the land surface of India had a relatively small influence on the monsoon climate, whereas the climate of China was found to be sensitive to the presence of vegetation cover. Crucifix et al. (2005) analysed the impact of vegetation variability on climate simulated with an atmosphere-slab ocean version of the Hadley Centre climate model coupled to a dynamic global vegetation model. Their results suggested that the impact of inter-annual vegetation variability on boundary layer potential temperature and relative humidity were small, implying that precipitation persistence was not strongly modified by vegetation dynamics in this model. This simulated weak coupling between vegetation and climate variability was attributed to a greater intrinsic variability in this model, overriding the effects of vegetation on the variability of surface fluxes. However, they pointed out that the weak coupling strength between surface fluxes and precipitation in this model (Koster et al., 2004) might have also contributed to the weak vegetation-climate coupling.

An afforestation study by Swann et al. (2012) documents the process by which northern extra-tropical vegetation can perturb tropical circulation. In their study they replaced grass and cropland with forest for the zonal band bounded by 30° N and 60° N in a version of the National Center for Atmospheric Research (NCAR) Community Atmosphere and Land models. The reduced albedo of the forests resulted in greater solar heating of the surface resulting in a net warming of the Northern Hemisphere , particularly in regions with low water availablity, and a northward shift in the tropical rain bands. Their result is consistent with expectation from idealised studies such as Broccoli et al. (2006) and Kang et al. (2008), who also document shifts of the ITCZ toward an anomalously warm hemisphere. Swann et al. (2012) demonstrate that relatively large perturbations to Northern Hemisphere vegetation cover are capable of producing a similar effect. A northward shift in the thermal equator and ITCZ in response to additional Northern Hemisphere extra-tropical warming is also found in Johns et al. (2003). In this case in response to anthropogenically forced climate change scenario.

A key feature of the analysis presented in this manuscript that differs from previous studies is that rather than idealised or hypothetical scenarios we utilise a number of existing alternative representations of present day vegatation cover, and one future scenario in HadCM3 simulations to demonstrate that the differences in these land cover data for HadCM3 can also have significant systematic impact on the simulation of large-scale tropical circulation and the Asian monsoon. These impacts can be of similar or greater magnitude to the uncertainty sampled by a perturbed physics ensemble of the same model. As a potential source of systematic bias this may be of particular relevance for multi-model experiments that co-ordinate land use classification, and in the evaluation of the tropical response to climate change in the latest generation of Earth system models.

2 HadCM3 model and data

2.1 Model description

This study compares the results from transient climate simulations of the Hadley Centre climate model (HadCM3, Pope et al., 2000; Gordon et al., 2000). This is an ocean-atmosphere general circulation model (GCM). The atmospheric component of HadCM3 is a hydrostatic grid-point model with a regular grid of 3.75° longitude by 2.5° latitude, approximately comparable to a T42 spectral resolution (Pope et al., 2000). In this study we utilize a version of HadCM3 incorporating both carbon cycle and dynamic vegetation components first documented in Cox et al. (2000). In contrast to the standard HadCM3 configuration this model uses version 2 of the Met Office surface exchange scheme (MOSES2, Essery et al., 2001) with a tiled representation of sub-grid scale heterogeneity, and is coupled to the Top-down Representation of Interactive Foliage and Flora Including Dynamics (TRIFFID) dynamic global vegetation model (DGVM, Cox, 2001). This allows both biogeophysical (photosynthesis) and biogeochemical (carbon cycle) feedbacks between the terrestrial biosphere and the atmosphere. The model also includes an interactive sulphur cycle component (Jones et al.,

2001) within the standard HadCM3 resolution. The model configuration was the unperturbed member of an ensemble of 17 parameter-perturbation experiments that were individually flux corrected for sea surface temperature and salinity, which minimised the regional temperature biases produced by this model across the ensemble. For the purposes of this analysis the flux adjustment means that climatological sea surface temperature differences between the model experiments are constrained to be small. The basis experiment (Booth and Jones, 2011) was run for two periods historical (1860–1989) and a future business as usual scenario (1989–2100) based on the A1B SRES scenario (Nakićenović et al., 2000) using non-CO_2 forcings as described by Johns et al. (2003).

2.2 Vegetation description

The standard vegetation distribution used in HadCM3 is derived from the global land use data of Wilson and Henderson-Sellers (1985) (hereafter WHS), but the MOSES2 configuration uses data derived from the International Geosphere-Biosphere Programme (IGBP) DISCover land-cover dataset (Loveland et al., 2000). This dataset uses information from the Advanced Very High Resolution Radiometer (AVHRR) data to define 14 land-cover classes at 1 km resolution (Hansen et al., 2000). The mapping between these classes and assumed fractions of the MOSES2 surface types are given in Essery et al. (2003). TRIFFID simulates the carbon uptake of, and competition between, five plant functional types (PFTs): broadleaf tree, needleleaf tree, C_3 grass, C_4 grass, and shrubs. Stomatal conductance and photosynthesis are calculated via a coupled leaf-level model, with leaf area index estimated from a percentage of the whole-plant carbon balance. Net primary productivity (NPP) is the difference between the simulated photosynthesis and dark respiration, with photosynthesis coupled to transpiration. NPP increases with CO_2 and also responds to temperature, photosynthetically active radiation (PAR), humidity, and soil moisture stress (Cox, 2001). The TRIFFID model therefore provides an alternative representation of global vegetation cover. WHS is the standard vegetation ancillary for HadCM3, so we will use WHS as our basis for comparison. We do not make any comment on the quality or biases in the WHS or IGBP datasets, instead they are used in experiments to demonstrate the sensitivity of HadCM3 atmospheric dynamics to these alternative representations of present day vegetation cover.

2.3 Experiment description

The basis experiment is the unperturbed member of the HadCM3 ensemble described above and in more detail in Booth and Jones (2011) and Booth et al. (2012), the experiment is free running from the year 1859 and includes the TRIFFID DGVM and estimates of historical forcings from natural and anthropogenic sources (Booth et al., 2012), and from model year 1989 to 2100 applies CO_2 emissions and other forcings from the A1b scenario (Nakićenović et al., 2000). Two additional 30 yr experiments were initialised from the atmospheric model state of this run in December 1959. These experiments had the vegetation cover and properties initialised to the equivalent estimates from WHS and IGBP as described above. In these experiments both the TRIFFID model and leaf-phenology model were switched off but in all other respects the model configuration is identical to that of Booth and Jones (2011). The experiments were run through to model year 1990, and the first year discarded from subsequent analysis to allow for any spinup resulting from the imposed vegetation change. All comparisons presented are therefore for the period of model years 1961 to 1990 inclusive.

In order to quantify any contribution from the dynamical components of TRIFFID and leaf phenology the set of experiments were repeated with the TRIFFID model switched off, but the leaf phenology module switched on. Therefore, the vegetation cover did not change, but leaf area index did. The experiments were identical in all other respects to those above with either the vegetation cover from a snapshot of the TRIFFID vegetation in 1959, WHS, or IGBP. The results from this repeat set of experiments were very similar to those with leaf phenology switched off so we conclude that the leaf phenology has no significant impact on the responses documented in this analysis, consistent with Lawrence and Slingo (2004), and providing confidence that the model response is indeed to the imposed change in vegetation cover and not the seasonality. We therefore treat each pairing of experiments as a 60 yr sample for the nominal present day climate state (model years 1961–1990) for each of the three descriptions of vegetation cover and refer to the combined sets hereafter as TRIF, WHS, and IGBP, respectively.

A fourth description of vegetation is taken as a snapshot of the vegetation from the TRIFFID DGVM in model year 2100 in the Booth et al. (2012) transient climate change experiment. Large perturbations to the tropical rainforests in response to climate change occur under the future simulation, but in this experiment we are particularly interested in quantifying sensitivity of tropical climate to Northern Hemisphere extra-tropical vegetation changes so we only impose the future changes to land areas north of 20° N. This experiment was run for the same period and is hereafter referred to as the TRIFfut experiment.

Differences between the vegetation cover estimates from WHS, IGBP, TRIF, and TRIFfut are shown in Fig. 1 for total vegetation cover and the needleaf (NL) tree classification. Equivalent plots to show the differences in other vegetation types are provided in Fig. S1 of the Supplement. Overall TRIF has more vegetation than WHS and IGBP has less. However, relative to WHS both TRIF and IGBP show some shifts in the needleaf forest cover over the northern mid-latitudes, a point that will be revisited in the discussions below. In TRIFfut tree cover expansion in the northern

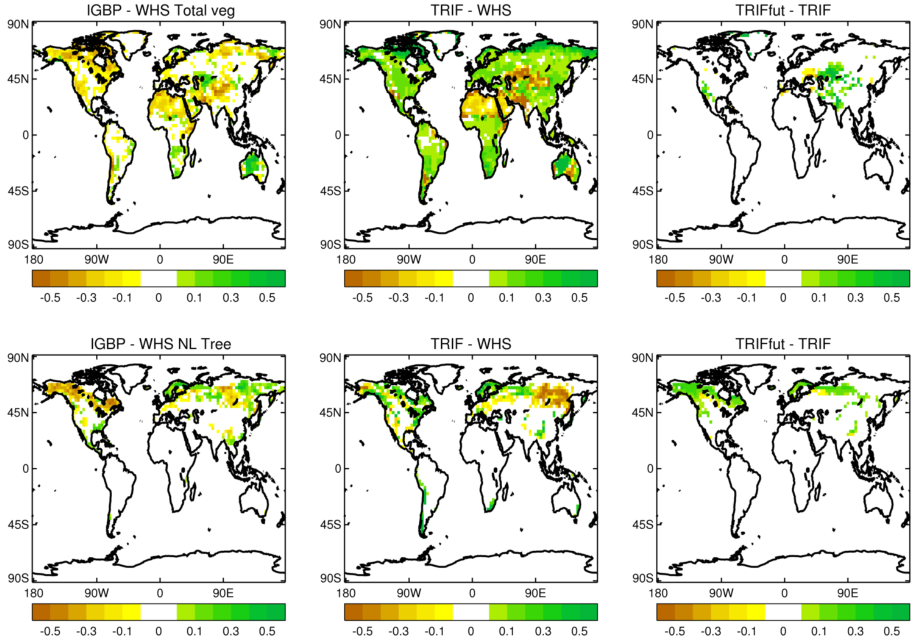

Fig. 1. Difference in vegetation cover (as a fraction of each model grid cell) compared to WHS of (left panel) IGBP and (middle) TRIF and between (right panel) TRIFfut and TRIF. The upper row represents the difference in total vegetation, and the lower row to (NL) needleleaf trees.

midlatitudes displaces shrub and grass (see Supplement) so the additional NL trees in the lower right panel of Fig. 1 are a shift from one vegetation type to another and therefore do not affect the total vegetation shown in the upper right panel of the same figure.

3 Climate response to vegetation distribution

3.1 Global response

Vegetation in the model affects surface properties particularly albedo and roughness, and is a crucial component of the surface hydrology affecting infiltration into the soil and transpiration into the atmosphere, as well as snow cover and snow melt. In the upper panel of Fig. 2 the net impact of the surface vegetation changes on the total upwelling shortwave (SW) at the top of the atmosphere (TOA) is shown. The all-sky diagnostic on the left is positive upward, so positive values indicate a higher proportion of reflected SW leaving the climate system. The central panel represents the clear-sky only contribution which will be dominated by changes in the surface albedo, the difference of all-sky and clear-sky in the right hand panel then provides the contribution from cloud radiative effects in the SW. The total upwelling SW is generally higher for the northern midlatitudes in both TRIF and IGBP, except for latitudes north of 60° N in TRIF. With the dominant contribution being from the clear-sky response, and a smaller overall contribution from cloud radiative effects (CRE). The changes in the mid-high latitudes are largely a consequence of changes in the surface albedo in response to the imposed vegetation change. Conversely, in the tropics the change in upwelling SW is a consequence of a southward shift in the tropical rain band dominated by the response in CRE, with much smaller response in the clear-sky diagnostic.

The zonal mean perturbations to temperature, precipitation, and 200 hPa winds resulting from changes to vegetation cover are presented in the lower panel of Fig. 2 as a gauge of the thermal, hydrological, and dynamical impacts of the vegetation change, respectively. Compared to the climate associated with WHS both IGBP (black line in Fig. 2) and TRIF (blue line in Fig. 2) experiments show a cooling of the Northern Hemisphere sub tropics and mid-latitudes consistent with the areas of higher albedo described above. At higher latitudes (60° N) the TRIF experiment shows a net warming. There is a southward shift in the inter-tropical convergence zone (ITCZ) seen in precipitation in the lower-middle panel of Fig. 2. The 200 hPa wind speed shows a dynamical response through a strengthening of the subtropical jets. The difference between TRIFfut and TRIF (red lines in Fig. 2) show essentially a similar but opposite pattern, suggesting that the imposed vegetation changes in this case work to offset the differences between TRIF and WHS. In the case of TRIFfut only the regions north of 20° N are changed, providing strong evidence that the tropical response in the ITCZ and jet streams are in response to extra-tropical vegetation change.

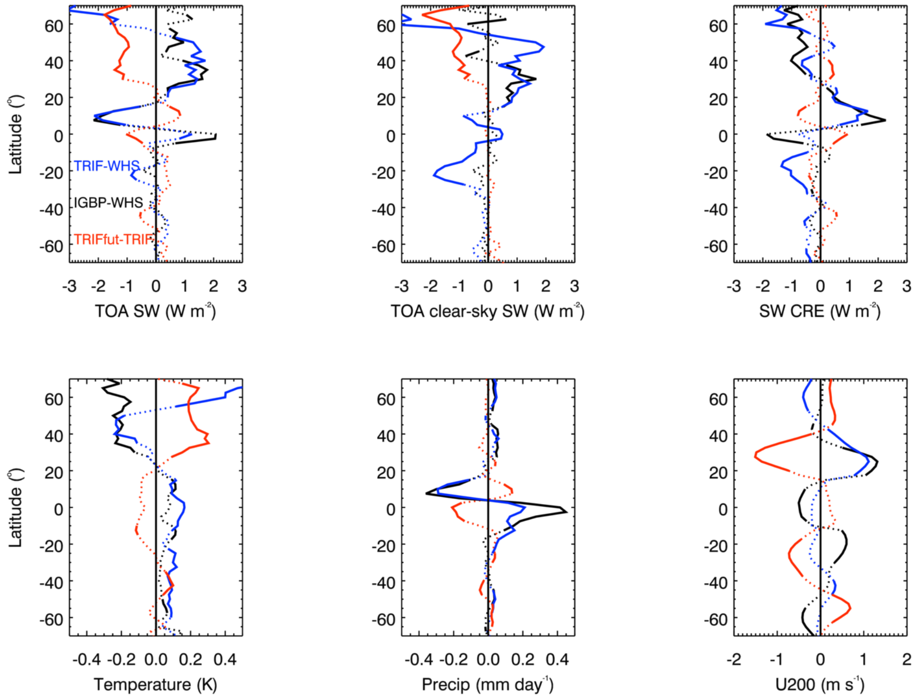

Fig. 2. Climate impact of imposed vegetation for (upper left panel) top of atmosphere (TOA) shortwave (SW), (upper middle panel) TOA clear sky only SW, (upper right panel) Cloud radiative effect in SW, (lower left panel) near surface air temperature, (lower middle panel) precipitation, and (lower right panel) 200 hPa zonal wind. The zonal mean differences between (black) IGBP-WHS, (blue) TRIF-WHS, and (red) TRIFfut-TRIF are shown. Unbroken segments represent regions where the difference is statistically significant at the 5 % level based on a student's t-test, while dotted segments are not significant.

The spatial pattern of change is shown in more detail in Fig. 3. Temperature changes are largest in the mid and high latitudes of the Northern Hemisphere, while the largest dynamical response is in the tropics. Although vegetation is also changed in the Southern Hemisphere in these experiments, the impact of those changes are relatively small compared to the north. Feedbacks within the model are also important, for example the change in vegetation through both cooling and change in surface roughness, which have a significant impact on the winter snow cover in the Northern Hemisphere, even though the precipitation is unaffected. The darker tree cover tends to reduce snow cover and the higher roughness of tall trees increase snow melt rates (Essery et al., 2001) further influencing the impact of the vegetation change on the surface albedo and temperature. Zonal mean and maps for each season equivalent to Figs. 2, 3 and Figs. S2 and S3 (available in the Supplement). A similar response is seen through all seasons although both the northern snow cover anomalies and the tropical circulation differences peak during the boreal spring.

There is considerable evidence from both paleoclimate and modelling studies that Northern Hemisphere cooling for example during glacial periods, results in a southward shift in the ITCZ. Broccoli et al. (2006) and Kang et al. (2008) conducted idealised model studies imposing anomalous coolingto the Northern Hemisphere and warming of the south. These simulations resulted in a shift of the ITCZ toward the warmer hemisphere. While the increased poleward eddy energy flux from the tropics induces a shift in the ITCZ, Kang et al. (2008, 2009) go on to demonstrate the importance and complicating influence of cloud and water vapour feedbacks, and the sensitivity of the tropical response to the parametrisation of entrainment within convective plumes. The results presented in Fig. 2 are broadly consistent with these previous studies and that of Swann et al. (2012) although the maximum cooling is further south, and over land in these simulations compared to the idealised experiments of Kang et al. (2008) and include a marked cooling of the subtropics. The simulations presented here provide further evidence that the representation of vegetation distribution within HadCM3 can produce sufficiently large perturbations to the surface climate to induce changes to the global hydrological cycle and large scale dynamics, particularly in the tropics.

A majority of the temperature and snow perturbations shown in Fig. 3 can be related to the specific change in needleaf trees between the experiments, and this is demonstrated for individual gridcells as a scatter plot in Fig. 4. So these experiments are suggesting that the climate response seen here is not sensitive to the total vegetation cover which

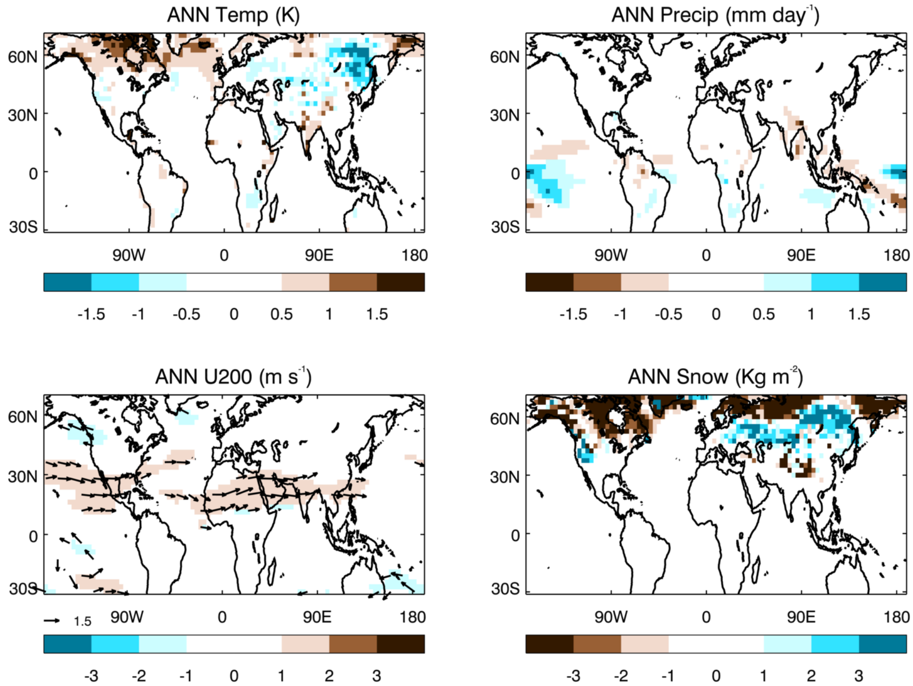

Fig. 3. Regional differences between TRIF and WHS for annual means of (upper left) temperature, (upper right panel) precipitation, (lower left panel) 200 hPa zonal wind, and (lower right panel) snow cover. The wind vector anomalies are also included in the U200 plots.

differs substantially between the IGBP and TRIF experiments (Fig. 1), but that it is more likely sensitive to changes in the effective surface albedo resulting from changes in mid-latitude needleleaf tree cover (Fig. 1).

3.2 Regional response

The regional pattern of change for boreal winter and summer are shown in Fig. 3 for the case of TRIF minus WHS. Temperature reductions are concentrated over much of the Eurasian continent, and increases are found over the Canadian Arctic. In contrast the precipitation and upper level wind anomalies tend to be larger over the oceans and reflect the shift in the ITCZ and modifications to the subtropical jet discussed above. During summer there is also a marked weakening of the tropical easterly jet over Africa (see Supplement) and reductions in precipitation over the Indian sub-continent. This summer rainfall deficit over India during the summer monsoon is the largest impact of the vegetation changes to land precipitation. The global perturbations described above, and the weakening of the tropical easterly jet, indicates the response is most likely a perturbation to the dynamical South Asian monsoon system rather than through local vegetation feedbacks over India itself, although additional local land-surface feedbacks cannot be entirely ruled out from these experiments.

One possible mechanism through which the mid and high latitude vegetation can induce these changes is through snow feedbacks. Figure 3 shows that the TRIF experiments have greater snow cover over the Eurasian continent which persist through both the the boreal winter and spring (Supplement). The pattern of snow cover change is largely related to the change in needleaf tree cover in the lower panel of Fig. 4.

3.3 The South Asia monsoon

Changes in precipitation and dynamical indices of the South Asian monsoon are shown in Fig. 5. All India precipitation is determined from land only model gridcells over India. The June to September mean all India precipitation in WHS, IGBP, and TRIF are 5.1 mm day^{-1}, 4.4 mm day^{-1} and 4.0 mm day^{-1}, respectively. In comparison the perturbed parameter ensemble of Booth et al. (2012) has an ensemble range of all India precipitation for the same season of 3.4 mm day^{-1} to 4.2 mm day^{-1}, demonstrating that the vegetation cover sensitivities demonstrated here are outside the range represented by the perturbed physics ensemble that uses the TRIFFID DGVM. The difference between the two "observed" land cover datasets of WHS and IGBP also differ by 0.7 mm day^{-1} comparable to the 0.8 mm day^{-1} range sampled by the perturbed physics ensemble.

The dynamical monsoon index of Wang et al. (2001, hereafter W01) compares 850 hPa zonal wind speeds in a region bounded by 5° N to 15° N, and 40° E to 80° E with those from 20° N to 30° N, and 60° E to 90° E while the index of Xavier et al. (2007, hereafter X07) is a thermodynamic index related to the north–south tropospheric heat source, and is calculated as the difference between the bulk temperature

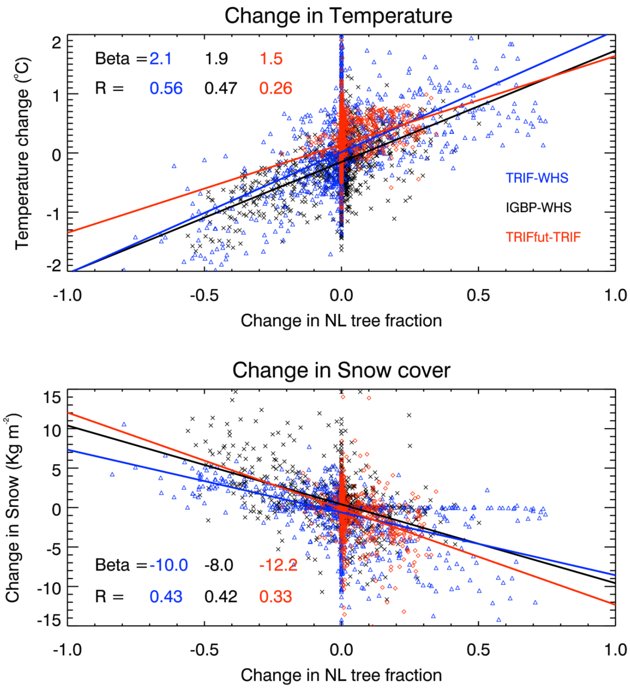

Fig. 4. Change in gridcell annual mean (top panel) temperature and (bottom panel snow cover against change in needleleaf (NL) tree cover in the grid box for (black) IGBP – WHS, (blue) TRIF – WHS, and (red) TRIFfut –TRIF. Values for the slope (Beta) and correlation coefficient (R) are given in each case.

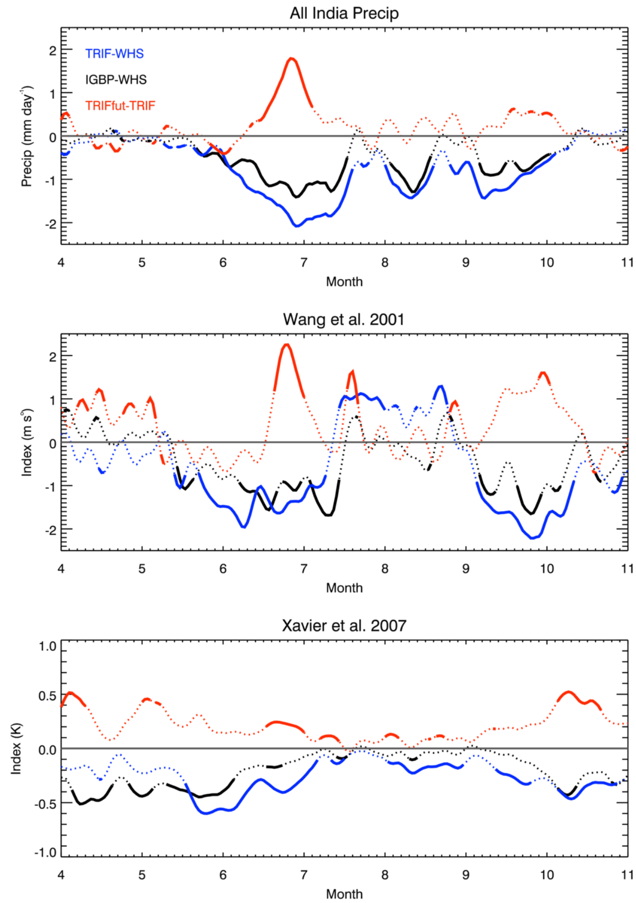

Fig. 5. Differences in the seasonal cycle of (top panel) all India precipitation, (middle) Indian monsoon index of W01, and (bottom panel) the index X07. Differences are presented as (black) IGBP – WHS, (blue) TRIF – WHS, (red) TRIFfut – TRIF. Unbroken segments represent times of year when the difference is statistically significant at the 5 % level based on a student's t-test, while dotted segments are not significant.

between 600 hPa and 200 hPa for a northern box bounded by 5° N to 35° S to 5° S, and 40° E to 100° E. Other indices such as Goswami et al. (1999) and Webster and Yang (1992) have been evaluated and support the general points dicussed below, but the three indices relating to all India precipitation, W01 and X07 are shown in Fig. 5 to summarise the hydrological, dynamic, and thermal response of the Asian monsoon system.

The greatest impact on precipitation (upper panel of Fig. 5) is seen during late June and early July where IGBP and TRIFFID vegetation both induce significant reductions to the strength of the low level jet (not shown) and all India rain. A generally diminishing precipitation anomaly then persists through the rest of the monsoon season. For the case of TRIFfut minus TRIF the precipitation is increased in TRIFfut for a relatively short period in late June. The W01 index also shows greatest difference during the months of June and September, indicating that the low level circulation is affected primarily during the onset and decay phases of the monsoon, although an increase in the W01 during July and August is seen in the TRIF experiment. A reduction of the tropospheric heat index of X07 is apparent in the monsoon onset. Defining the onset and withdrawal dates of the monsoon for X07 as the dates at which the index becomes positive (indicating the reversal of the medridional temperature gradient), the onset is delayed by an average of 6 days in TRIF relative to WHS and the duration is reduced by 8 days, further supporting that the main response is during the onset and early monsoon.

Discussions of extra-tropical forcing of the South Asian monsoon have been ongoing for more than one hundred years (Blandford, 1884), with particular interest paid to the role of Eurasian and Himalayan winter snow cover in modifying the subsequent summer monsoon, (e.g. Peings and Douville, 2010, and references therein). The potential for vegetation to induce such impacts has also been documented in studies of the Last Glacial Maximum (Crucifix and Hewitt, 2005) with somewhat more extreme vegetation changes than are considered here. Furthermore, the importance of the boreal forests has been highlighted within a number of studies (e.g. Bonan et al., 1992; Douville and Royer, 1996), but a more recent study by Peings and Douville (2010) questions the robustness of the snow-monsoon link, particularly due to apparent complicating influence of El Niño and Southern Oscillation variability (Fasullo, 2004). However, a recent study by Turner and Slingo (2011) demonstrate the teleconnection does exist within the HadCM3 model by using idealised snow forcing experiments. They demonstrate the importance of the Himalayas and Tibetan Plateau in reducing meridional tropospheric temperature gradients largely through snow albedo feedbacks resulting in a weakening of the early monsoon. Compared to WHS the IGBP and TRIF experiments both have significant cold anomalies during winter and Spring through much of Eurasia, the middle East, and parts of the Tibetan Plateau, but in contrast to Turner and Slingo (2011) the consistent response is greatest over the mid to high latitudes than over the Tibetan Plateau. The U200 anomalies in Fig. 3 for DJF and MAM also show a strengthening of the subtropical jet during DJF and MAM that is a potential pre-cursor to a weak monsoon (Yang et al., 2004). While it is not possible with these experiments to distinguish the potential role of the Tibetan plateau, or Boreal forests specifically through thermal, and dynamical feedbacks, the simulated responses are broadly consistent with these well studied mechanisms, which therefore represent the most likely processes by which the south Asian monsoon in HadCM3 exhibits sensitivity to the choice of present day Northern Hemisphere vegetation, particularly needleleaf tree cover.

The difference between TRIFfut and TRIF (red line in Fig. 5) shows a similar pattern but in the opposite sense. The simulated change in extra-tropical vegetation by the TRIFFID DGVM for the 21st century has a positive impact on the strength of the South Asian monsoon in that simulation, through similar processes to those that contribute to the large-scale tropical climate perturbations discussed above. The increase in needleaf tree cover for this experiment is shown in the lower right panel of Fig. 1. The greatest impact on the simulated land precipitation occurring during the monsoon onset, which is again consistent with a snow forcing, as these do not persist into the boreal summer season (Turner and Slingo, 2011). Within the transient climate change scenario these vegetation feedbacks would interact with other land surface (e.g. snow albedo) and atmospheric climate feedbacks.

4 Conclusions

In this paper we have demonstrated a sensitivity of HadCM3 tropical climate to extra-tropical vegetation changes resulting from the use of broadly similar, but different, land use datasets. The resulting dynamical response and impact on the south Asian summer monsoon in particular are consistent with numerous previous studies in both the HadCM3 model and other GCMs, resulting from changes in midlatitude temperatures and snow albedo feedbacks, affecting in particular the onset of the summer south Asian monsoon. This study does not offer any new insights into these teleconnection processes specifically, but rather serves to demonstrate how the representation of vegetation, and uncertainties associated with correctly doing so, can have significant implications for the representation of tropical climates in this model. Feddema et al. (2005) presented a similar argument based on an analysis of the impact of land cover change on the NCAR-DOE PCM. HadCM3 has previously been noted for having a relatively weak surface-atmosphere coupling in a comparison of twelve GCMs (Koster et al., 2004), yet still large-scale dynamical responses can result from uncertainty in vegetation classifications, particularly in the northern boreal forests.

With the emergence and continued development of earth system models to explore both 21st century climate change, and reconstruct paleo-climates, due consideration should be made for the potentially important role that extra-tropical vegetation feedbacks might have on tropical climate change and its uncertainty. Idealised experiments such as those of Kang et al. (2008) and Turner and Slingo (2011) identify the dynamical mechanisms for key feedbacks in individual GCMs, but the representation of these teleconnections may not be consistent across different climate models (Peings and Douville, 2010). In order to compare the outcomes of different climate models it is desirable to use common land use classification, as adopted by Hurtt et al. (2011), but here we demonstrate that systematic biases in the simulated climate may be introduced through choice of vegetation cover and that alternative estimates of not just future but also present day land use and vegetation properties are desirable for exploring the wider importance of the terrestrial biosphere in GCMs, not just for regional detail of surface–atmosphere interaction but also for its contribution to large-scale atmospheric teleconnections.

Supplementary material related to this article is available online at: http://www.earth-syst-dynam.net/3/87/2012/esd-3-87-2012-supplement.pdf.

Acknowledgements. This study was carried out under the collaborative program between IITM and Met Office UK and the contribution of J. Sanjay was conducted during his time as a visiting scientist at the Met Office Hadley Centre. The contribution of Met Office authors was supported by the Joint DECC and Defra Integrated Climate Programme –DECC/Defra (GA01101).

Edited by: A. Kleidon

References

Blandford, H. F.: On the connection of Himalayan snowfall with dry winds and seasons of drought in India, P. Roy. Soc. Lond., 37, 3–22, 1884.

Bonan, G. B., Pollard, D., and Thompson, S. L.: Effects of boreal forest vegetation on global climate, Nature, 359, 716–718, doi:10.1038/359716a0, 1992.

Booth, B. B. B. and Jones, C. D.: Terrestrial response of QUMPC ensemble, Tech. Rep. 89, Met Office, http://www.metoffice.gov.uk/learning/library/publications/science/climate-science, last access: October 2011.

Booth, B. B., Jones, C. D., Collins, M., Totterdell, I. J., Cox, P. M., Sitch, S., Huntingford, C., Betts, R. A., Harris, G. R., and Lloyd, J.: High sensitivity of future global warming to land carbon cycle processes, Environ. Res. Lett., 7, 024002, doi:10.1088/1748-9326/7/2/024002, 2012.

Broccoli, A. J., Dahl, K. A., and Stouffer, R. J.: Response of the ITCZ to Northern Hemisphere cooling, Geophys. Res. Lett., 33, L01702, doi:10.1029/2005GL024546, 2006.

Cox, P. M.: Description of the "TRIFFID" Dynamic Global Vegetation Model, Tech. Rep. 24, Met Office, http://www.metoffice.gov.uk/learning/library/publications/science/climate-science/hadley-centre-technical-note (last access: October 2011), 2001.

Cox, P. M., Betts, R. A., Spall, S. A., and Totterdell, I. J.: Acceleration of global warming due to carbon-cycle feedbacks in a coupled climate model, Nature, 408, 184–187, doi:10.1038/35041539, 2000.

Crucifix, M. and Hewitt, C.: Impact of vegetation changes on the dynamics of the atmosphere at the Last Glacial Maximum, Clim. Dynam., 25, 447–459, doi:10.1007/s00382-005-0013-8, 2005.

Crucifix, M., Betts, R. A., and Cox, P. M.: Vegetation and climate variability: a GCM modelling study, Clim. Dynam., 24, 457–467, doi:10.1007/s00382-004-0504-z, 2005.

Denman, K. L., Brasseur, G., Chidthaisong, A., Ciais, P., Cox, P. M., Dickinson, R. E., Hauglustaine, D., Heinze, C., Holland, E., Jacob, D., Lohmann, U., Ramachandran, S., da Silva Dias, P. L., Wofsy, S. C., and Zhang, X.: Couplings Between Changes in the Climate System and Biogeochemistry, in: Climate Change 2007: The Physical Science Basis, Contribution of Working Group I to the Fourth Assessment Report of the Intergovernmental Panel on Climate Change, edited by: Solomon, S., Qin, D., Manning, M., Chen, Z., Marquis, M., Averyt, K. B., Tignor, M., and Miller, H. L., chap. 7, Cambridge University Press, Cambridge, UK and New York, NY, USA, 2007.

Douville, H. and Royer, J.: Sensitivity of the Asian summer monsoon to an anomalous Eurasian snow cover within the Météo-France GCM, Clim. Dynam., 12, 449–466, doi:10.1007/BF02346818, 1996.

Essery, R., Best, M. J., and Cox, P.: MOSES 2.2 Technical Documentation, Tech. Rep. 30, Met Office, http://www.metoffice.gov.uk/learning/library/publications/science/climate-science/hadley-centre-technical-note (last access: October 2011), 2001.

Essery, R. L. H., Best, M. J., Betts, R. A., Cox, P. M., and Taylor, C. M.: Explicit Representation of Subgrid Heterogeneity in a GCM Land Surface Scheme, J. Hydrometeorol., 4, 530–543, doi:10.1175/1525-7541(2003)004<0530:EROSHI>2.0.CO;2, 2003.

Fasullo, J.: A Stratified Diagnosis of the Indian Monsoon-Eurasian Snow Cover Relationship, J. Climate, 17, 1110–1122, doi:10.1175/1520-0442(2004)017<1110:ASDOTI>2.0.CO;2, 2004.

Feddema, J., Oleson, K., Bonan, G., Mearns, L., Washington, W., Meehl, G., and Nychka, D.: A comparison of a GCM response to historical anthropogenic land cover change and model sensitivity to uncertainty in present-day land cover representations, Clim. Dynam., 25, 581–609, doi:10.1007/s00382-005-0038-z, 2005.

Friedlingstein, P., Cox, P., Betts, R., Bopp, L., von Bloh, W., Brovkin, V., Cadule, P., Doney, S., Eby, M., Fung, I., Bala, G., John, J., Jones, C., Joos, F., Kato, T., Kawamiya, M., Knorr, W., Lindsay, K., Matthews, H. D., Raddatz, T., Rayner, P., Reick, C., Roeckner, E., Schnitzler, K. G., Schnur, R., Strassmann, K., Weaver, A. J., Yoshikawa, C., and Zeng, N.: Climate-Carbon Cycle Feedback Analysis: Results from the C4MIP Model Intercomparison, J. Climate, 19, 3337–3353, doi:10.1175/JCLI3800.1, 2006.

Gallimore, R., Jacob, R., and Kutzbach, J.: Coupled atmosphere-ocean-vegetation simulations for modern and mid-Holocene climates: role of extratropical vegetation cover feedbacks, Clim. Dynam., 25, 755–776, doi:10.1007/s00382-005-0054-z, 2005.

Gordon, C., Cooper, C., Senior, C. A., Banks, H., Gregory, J. M., Johns, T. C., Mitchell, J. F. B., and Wood, R. A.: The simulation of SST, sea ice extents and ocean heat transports in a version of the Hadley Centre coupled model without flux adjustments, Clim. Dynam., 16, 147–168, doi:10.1007/s003820050010, 2000.

Goswami, B. N., Krishnamurthy, V., and Annmalai, H.: A broad-scale circulation index for the interannual variability of the Indian summer monsoon, Q. J. Roy. Meteorol. Soc., 125, 611–633, doi:10.1002/qj.49712555412, 1999.

Hansen, M. C., Defries, R. S., Townshend, J. R. G., and Sohlberg, R.: Global land cover classification at 1 km spatial resolution using a classification tree approach, Int. J. Remote Sens., 21, 1331–1364, doi:10.1080/014311600210209, 2000.

Hurtt, G., Chini, L., Frolking, S., Betts, R., Feddema, J., Fischer, G., Fisk, J., Hibbard, K., Houghton, R., Janetos, A., Jones, C., Kindermann, G., Kinoshita, T., Klein Goldewijk, K., Riahi, K., Shevliakova, E., Smith, S., Stehfest, E., Thomson, A., Thornton, P., van Vuuren, D., and Wang, Y.: Harmonization of land-use scenarios for the period 1500–2100: 600 years of global gridded annual land-use transitions, wood harvest, and resulting secondary lands, Climatic Change, 109, 117–161, doi:10.1007/s10584-011-0153-2, 2011.

Johns, T. C., Gregory, J. M., Ingram, W. J., Johnson, C. E., Jones, A., Lowe, J. A., Mitchell, J. F. B., Roberts, D. L., Sexton, D. M. H., Stevenson, D. S., Tett, S. F. B., and Woodage, M. J.: Anthropogenic climate change for 1860 to 2100 simulated with the HadCM3 model under updated emissions scenarios, Clim. Dynam., 20, 583–612, doi:10.1007/s00382-002-0296-y, 2003.

Jones, A., Roberts, D. L., Woodage, M. J., and Johnson, C. E.: Indirect sulphate aerosol forcing in a climate model with an interactive sulphur cycle, J. Geophys. Res., 106, 20293–20310, doi:10.1029/2000JD000089, 2001.

Jones, C. D., Hughes, J. K., Bellouin, N., Hardiman, S. C., Jones, G. S., Knight, J., Liddicoat, S., O'Connor, F. M., Andres, R. J., Bell, C., Boo, K.-O., Bozzo, A., Butchart, N., Cadule, P., Corbin, K. D., Doutriaux-Boucher, M., Friedlingstein, P., Gornall, J., Gray, L., Halloran, P. R., Hurtt, G., Ingram, W. J., Lamarque, J.-F., Law, R. M., Meinshausen, M., Osprey, S., Palin, E. J., Parsons Chini, L., Raddatz, T., Sanderson, M. G., Sellar, A. A., Schurer, A., Valdes, P., Wood, N., Woodward, S., Yoshioka, M., and Zerroukat, M.: The HadGEM2-ES implementation of CMIP5 centennial simulations, Geosci. Model Dev., 4, 543–570, doi:10.5194/gmd-4-543-2011, 2011.

Kang, S. M., Held, I. M., Frierson, D. M. W., and Zhao, M.: The Response of the ITCZ to Extratropical Thermal Forcing: Idealized Slab-Ocean Experiments with a GCM, J. Climate, 21, 3521–3532, doi:10.1175/2007JCLI2146.1, 2008.

Kang, S. M., Frierson, D. M. W., and Held, I. M.: The Tropical Response to Extratropical Thermal Forcing in an Idealized GCM: The Importance of Radiative Feedbacks and Convective Parameterization, J. Atmos. Sci., 66, 2812–2827, doi:10.1175/2009JAS2924.1, 2009.

Koster, R. D., Dirmeyer, P. A., Guo, Z., Bonan, G., Chan, E., Cox, P., Gordon, C. T., Kanae, S., Kowalczyk, E., Lawrence, D., Liu, P., Lu, C.-H., Malyshev, S., McAvaney, B., Mitchell, K., Mocko, D., Oki, T., Oleson, K., Pitman, A., Sud, Y. C., Taylor, C. M., Verseghy, D., Vasic, R., Xue, Y., and Yamada, T.: Regions of Strong Coupling Between Soil Moisture and Precipitation, Science, 305, 1138–1140, doi:10.1126/science.1100217, 2004.

Lawrence, D. M. and Slingo, J. M.: An annual cycle of vegetation in a GCM, Part II: global impacts on climate and hydrology, Clim. Dynam., 22, 107–122, doi:10.1007/s00382-003-0367-8, 2004.

Levis, S., Bonan, G. B., and Bonfils, C.: Soil feedback drives the mid-Holocene North African monsoon northward in fully coupled CCSM2 simulations with a dynamic vegetation model, Clim. Dynam., 23, 791–802, doi:10.1007/s00382-004-0477-y, 2004.

Loveland, T. R., Reed, B. C., Brown, J. F., Ohlen, D. O., Zhu, Z., Yang, L., and Merchant, J. W.: Development of a global land cover characteristics database and IGBP DISCover from 1 km AVHRR data, Int. J. Remote Sens., 21, 1303–1330, doi:10.1080/014311600210191, 2000.

Malhi, Y., Aragão, L. E. O. C., Galbraith, D., Huntingford, C., Fisher, R., Zelazowski, P., Sitch, S., McSweeney, C., and Meir, P.: Exploring the likelihood and mechanism of a climate-change-induced dieback of the Amazon rainforest, P. Natl. Acad. Sci., 106, 20610–20615, doi:10.1073/pnas.0804619106, 2009.

Martin, G. M., Arpe, K., Chauvin, F., Ferranti, L., Maynard, K., Polcher, J., Stephenson, D. B., and Tschuck, P.: Simulation of the Asian summer monsoon in five European general circulation models, Atmos. Sci. Lett., 1, 37–55, doi:10.1006/asle.2000.0004, 2000.

Nakićenović, N., Alcamo, J., Davis, G., de Vries, B., Fenhann, J., Gaffin, S., Gregory, K., Grübler, A., Jung, T. Y., Kram, T., Lebre La Rovere, E., Michaelis, L., Mori, S., Morita, T., Pepper, W., Pitcher, H., Price, L., Riahi, K., Roehrl, A., Rogner, H. H., Sankovski, A., Schlesinger, M., Shukla, P., Smith, S., Swart, R., van Rooijen, S., Victor, N., and Dadi, Z.: IPCC Special Report on Emissions Scenarios (SRES), http://www.ipcc.ch/ipccreports/sres/emission/index.php?idp=0, last access: October 2011, Cambridge University Press, UK, 2000.

Osborne, T. M., Lawrence, D. M., Slingo, J. M., Challinor, A. J., and Wheeler, T. R.: Influence of vegetation on the local climate and hydrology in the tropics: sensitivity to soil parameters, Clim. Dynam., 23, 45–61, doi:10.1007/s00382-004-0421-1, 2004.

Peings, Y. and Douville, H.: Influence of the Eurasian snow cover on the Indian summer monsoon variability in observed climatologies and CMIP3 simulations, Clim. Dynam., 34, 643–660, doi:10.1007/s00382-009-0565-0, 2010.

Pope, V. D., Gallani, M. L., Rowntree, P. R., and Stratton, R. A.: The impact of new physical parametrizations in the Hadley Centre climate model: HadAM3, Clim. Dynam., 16, 123–146, doi:10.1007/s003820050009, 2000.

Swann, A. L. S., Fung, I. Y., and Chiang, J. C. H.: Mid-latitude afforestation shifts general circulation and tropical precipitation, P. Natl. Acad. Sci., 109, 712–716, doi:10.1073/pnas.1116706108, 2012.

Turner, A. and Slingo, J.: Using idealized snow forcing to test teleconnections with the Indian summer monsoon in the Hadley Centre GCM, Clim. Dynam., 36, 1717–1735, doi:10.1007/s00382-010-0805-3, 2011.

Turner, A. G. and Slingo, J. M.: Subseasonal extremes of precipitation and active-break cycles of the Indian summer monsoon in a climate-change scenario, Q. J. Roy. Meteorol. Soc., 135, 549–567, doi:10.1002/qj.401, 2009.

Wang, B., Wu, R., and Lau, K. M.: Interannual Variability of the Asian Summer Monsoon: Contrasts between the Indian and the Western North Pacific East Asian Monsoons, J. Climate, 14, 4073–4090, doi:10.1175/1520-0442(2001)014<4073:IVOTAS>2.0.CO;2, 2001.

Webster, P. J. and Yang, S.: Monsoon and Enso: Selectively Interactive Systems, Q. J. Roy. Meteorol. Soc., 118, 877–926, doi:10.1002/qj.49711850705, 1992.

Wilson, M. F. and Henderson-Sellers, A.: A global archive of land cover and soils data for use in general circulation climate models, J. Climatol., 5, 119–143, 1985.

Xavier, P. K., Marzin, C., and Goswami, B. N.: An objective definition of the Indian summer monsoon season and a new perspective on the ENSO monsoon relationship, Q. J. Roy. Meteorol. Soc., 133, 749–764, doi:10.1002/qj.45, 2007.

Yang, S., Lau, K. M., Yoo, S. H., Kinter, J. L., Miyakoda, K., and Ho, C. H.: Upstream Subtropical Signals Preceding the Asian Summer Monsoon Circulation, J. Climate, 17, 4213–4229, doi:10.1175/JCLI3192.1, 2004.